Rapid Communications

Spin Hall magnetoresistance in a low-dimensional Heisenberg ferromagnet

Saül Vélez,[1,2,*] Vitaly N. Golovach,[3,4,5,†] Juan M. Gomez-Perez,[1] Andrey Chuvilin,[1,5] Cong Tinh Bui,[6,7] F. Rivadulla,[6] Luis E. Hueso,[1,5] F. Sebastian Bergeret,[3,4,‡] and Fèlix Casanova[1,5,§]

[1]*CIC nanoGUNE, 20018 Donostia-San Sebastian, Basque Country, Spain*

[2]*Department of Materials, ETH Zürich, 8093 Zürich, Switzerland*

[3]*Centro de Física de Materiales (CFM-MPC), Centro Mixto CSIC-UPV/EHU, 20018 Donostia-San Sebastian, Basque Country, Spain*

[4]*Donostia International Physics Center (DIPC), 20018 Donostia-San Sebastian, Basque Country, Spain*

[5]*IKERBASQUE, Basque Foundation for Science, 48013 Bilbao, Basque Country, Spain*

[6]*Centro Singular de Investigación en Química Biolóxica e Materiales Moleculares (CiQUS), and Departamento de Química-Física, Universidad de Santiago de Compostela, 15782 Santiago de Compostela, Spain*

[7]*Department of Electrical and Electronic Engineering, Tokyo Institute of Technology, 2-12-1 Ookayama, Meguro, Tokyo 152-0033, Japan*

(Received 29 May 2018; revised manuscript received 13 August 2019; published 4 November 2019)

We report the spin Hall magnetoresistance (SMR) in Pt deposited on a tensile-strained $LaCoO_3$ (LCO) thin film, which is a ferromagnetic insulator with a Curie temperature $T_c = 85$ K. The SMR displays a strong magnetic-field dependence below T_c, with the SMR amplitude continuing to increase (linearly) with increasing the field far beyond the saturation value of the ferromagnet. The SMR amplitude decreases gradually with raising the temperature across T_c and remains measurable even above T_c. Moreover, no hysteresis is observed in the field dependence of the SMR. These unusual behaviors indicate that a low-dimensional magnetic system forms at the surface of LCO and that the LCO/Pt interface decouples magnetically from the rest of the LCO thin film. Transmission electron microscopy analysis of the heterostructure reveals that an ultrathin Co-rich layer forms at the LCO surface upon deposition of Pt, which is separated from the rest of the LCO film by a ∼1-nm La/O-rich layer, thus supporting the presence of a low-dimensional ferromagnetic system. To explain the magnetoresistance measurements, we revisit the derivation of the SMR corrections and relate the spin-mixing conductances to the spin-spin correlation functions and microscopic quantities describing the magnetism at the interface. Comparisons between theory and experiment confirm the existence of a low-dimensional Heisenberg ferromagnet at the interface. Our results pave the way for exploring complex magnetic textures of insulating films by simple transport measurements.

DOI: 10.1103/PhysRevB.100.180401

Introduction. Magnetoresistance has been key for understanding spin-dependent transport in solids [1]. In the last years, new magnetoresistance phenomena were discovered in thin ferromagnetic/normal metal (FM/NM)-based heterostructures [2–18], which originate from the interplay of the spin currents generated in the heterostructure (via the spin Hall effect [19–22] or the Rashba-Edelstein effect [23,24]) with the magnetic moments of the FM layer. Among many applications, these magnetoresistance effects have been used for quantifying spin transport properties such as the spin diffusion length λ and the spin Hall angle θ_{SH} of different NM layers, or the spin-mixing conductance $G_{\uparrow\downarrow}$ of FM/NM interfaces. More interestingly, unlike other surface-sensitive techniques that suffer from a bulk contribution due to a finite penetration depth, the spin Hall magnetoresistance (SMR) [4–11] uses the spin accumulation at interfaces for sensing the magnetic properties of the very first atomic layer of magnetic insulators (MIs) [25,26]. For instance, SMR has been employed for probing the surface of complex magnetic systems such as ferrimagnetic spinel oxides [11,48], spin-spiral multiferroics [49,50], canted ferrimagnets [51], $Y_3Fe_5O_{12}$/antiferromagnetic (YIG/AFM) bilayers [52,53], and synthetic AFMs [54].

$LaCoO_3$ (LCO) presents an intriguing magnetic behavior, which has been studied for decades and is still under debate [55–70]. Bulk LCO is a diamagnetic insulator at low temperature, owing to the low-spin (LS) configuration of Co^{3+}. The relatively small crystal-field splitting of the Co^{3+} $3d$ shell results in an increasing population of high-spin (HS) Co^{3+} with temperature, reaching 1:1 (LS:HS) above ∼150 K. The close proximity between crystal-field splitting and exchange energy makes the magnetic properties of LCO particularly susceptible to small changes in interionic distances and coordination. For this reason, tensile-strained LCO thin films grown on particular substrates [such as $SrTiO_3$ (STO)] exhibit FM order at low temperatures [63–70]. However, little is known regarding the surface magnetic properties of these films. Recent Hall measurements performed in strained LCO/Pt showed interesting and puzzling temperature and magnetic field behavior [71], but no connection with the magnetic properties of the LCO surface was made.

In this Rapid Communication, we study the magnetic properties of the surface of strained LCO films in contact

*saul.velez@mat.ethz.ch
†vitaly.golovach@ehu.eus
‡sebastian_bergeret@ehu.eus
§f.casanova@nanogune.eu

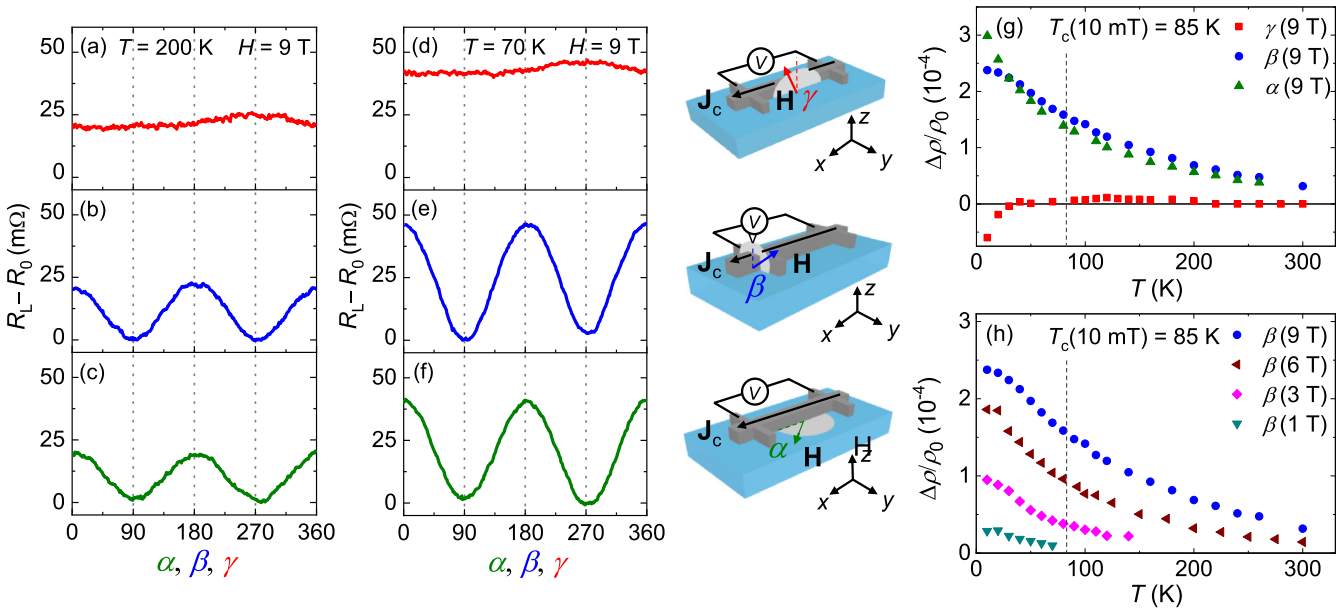

FIG. 1. Longitudinal ADMR measurements performed in LCO(19 nm)/Pt(7 nm) at (a)–(c) 200 K and (d)–(f) 70 K for $H = 9$ T in the α-, β-, and γ-rotation planes. The sketches indicate the definition of the angles, the axes, and the measurement configuration. R_0 is taken as $R_L(\alpha, \beta = 90^\circ)$. (g) Temperature dependence of the normalized ADMR amplitude, $\Delta\rho/\rho_0 \cong [R_L(0^\circ) - R_L(90^\circ)]/R_L(90^\circ)$, measured at 9 T in the α, β, and γ planes (the data are fitted to a $\cos^2$ dependence). ρ_0 is the Drude resistivity. (h) Temperature dependence of $\Delta\rho/\rho_0$ measured in the β plane for different H values. Vertical dashed lines in (g) and (h) indicate T_c of LCO at 10 mT [26].

with Pt by performing magnetotransport measurements. We find that the SMR depends strongly on the magnetic field at all temperatures, both above and below the Curie temperature (T_c) of the film, and, more strikingly, no hysteresis in the magnetoresistance is observed. These observations clearly show that the surface magnetism of the LCO film is radically different from its bulk counterpart. We support our measurements with a theoretical model that extends the known expressions for SMR [7,72] and HMR [73,74] in MI/NM bilayers for an arbitrary magnetic ordering (para-, ferri-, ferro-, antiferromagnetic) of the localized magnetic moments at the MI/NM interface. We provide expressions for $G_{\uparrow\downarrow} = G_r + iG_i$ [25,75] and the effective spin conductance G_s [76,77] in terms of surface spin correlators. The experimental data evidence that the surface of LCO behaves as a low-dimensional Heisenberg FM. Our interpretation is confirmed by scanning transmission electron microscopy (STEM) and electron energy loss spectroscopy (EELS), which reveals the formation of an ultrathin Co-rich layer at the LCO surface. These results demonstrate the predictive power of our model for analyzing the magnetic properties of surfaces when combined with magnetotransport measurements.

Experimental details. Growth of epitaxial LCO thin films via polymer-assisted deposition on (001) STO substrates, as well as their structural, electrical, and magnetic characterization are described in Ref. [67]. The LCO films exhibit a tetragonal distortion, which induces FM ordering below $T_c \sim 85$ K and with a coercive field below 1 T at 10 K [26,67], in agreement to other reports [64–66,68,71]. The films exhibit a low surface roughness (<1 nm) and are insulating [67]. Pt Hall bar structures (width $W = 100$ μm, length $L = 800$ μm, and thickness $d_N = 7$ nm) were patterned on top of the LCO films via e-beam lithography, sputtering deposition of Pt, and lift-off. Two samples with different LCO thicknesses, 12 and 19 nm, were prepared and studied, showing similar results. Below, we present data for the 19-nm-thick LCO film. Magnetotransport measurements were performed between 10 and 300 K in a liquid-He cryostat that allows applying magnetic fields H of up to 9 T and rotating the sample by 360°. The cross section of the heterostructure was analyzed by high-resolution high-angle annular dark field (HAADF) STEM and EELS on a Titan 60-300 electron microscope.

Longitudinal magnetoresistance in LCO/Pt. Figures 1(a)–1(f) show the longitudinal angular-dependent magnetoresistance (ADMR) in LCO/Pt at 200 and 70 K and for $H = 9$ T in the three relevant **H**-rotation planes α,β,γ (see sketches). We can see a clear ADMR with a $\cos^2$ modulation in α and β, and almost no variation in γ. These angular dependences are in agreement with the ones expected for spin-related magnetoresistances, such as SMR and HMR [5,74]. Surprisingly, this angular symmetry is not only observed below T_c of LCO [Figs. 1(d)–1(f)] but also above, i.e., when the LCO film is in the paramagnetic (PM) state [Figs. 1(a)–1(c)].

Figure 1(g) shows the temperature dependence of the ADMR amplitude measured at 9 T in the α, β, and γ planes. The amplitude is roughly the same in α and β and decays monotonously with temperature, whereas it is negligibly small in γ, except for very low temperatures. The sign of the ADMR in γ and the increase in α below ~20 K suggest the emergence of the magnetic proximity effect (MPE) at the LCO/Pt interface at low temperatures. The MPE could be at the origin of the unusual temperature dependence of the Hall resistance reported in this system [71], an unconventional behavior that is also observed in our sample [26].

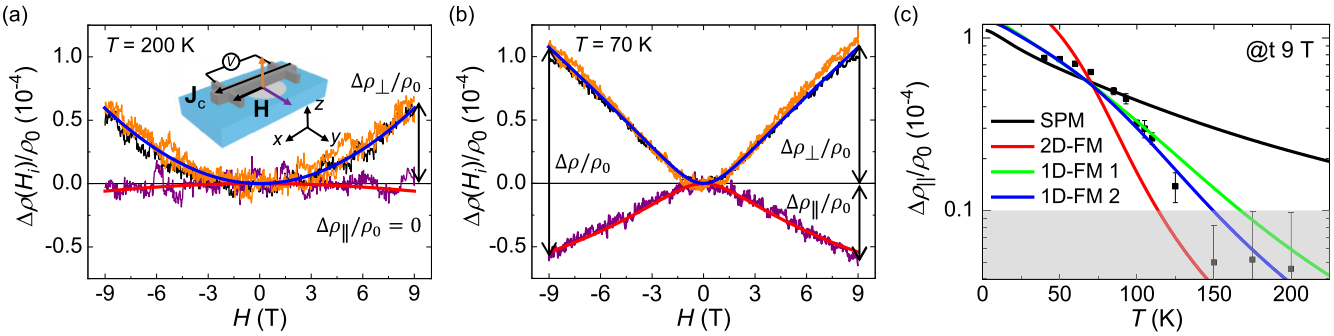

FIG. 2. (a), (b) Normalized FDMR measurements, $\Delta\rho(H_i)/\rho_0 \cong [R_L(H_i) - R_L(0)]/R_L(0)$ (H_i indicates the magnetic field applied along the i direction), performed in LCO(19 nm)/Pt(7 nm) at (a) 200 K and (b) 70 K along the three main sample axes. The sketch in (a) indicates the definition of the axes, the color code of the magnetic field direction, and measurement configuration. The red and blue lines are representative fits of the experimental data using Eqs. (2) and (3). The LCO surface is modeled as a plane of 1D-FM Co chains with $S = 3/2$, $n_s = 2.187 \times 10^{18}$ spins/m^2, and $J = 13.1$ meV, and used $\nu J_{sd} = -0.15$ (constant with T), $\theta_{SH} = 0.115(0.098)$, $\lambda = 4.00$ nm (4.72 nm), and $D = 70.9 \times 10^{-6}$ m^2 s^{-1} (83.7×10^{-6} m^2 s^{-1}) at 200 K (70 K). We assume $g = 2$. (c) Temperature dependence of $\frac{\Delta\rho_\parallel}{\rho_0}$ at 9 T [see (b) for its definition]. The shaded region indicates the noise floor. The square dots represent the experimental data and the solid lines are fits obtained modeling the LCO/Pt interface as a 2D and a 1D Heisenberg FM (2D-FM, red line, and 1D-FM 1, green line, respectively), as 1D-FM ladders (1D-FM 2, blue line), and as a SPM (black line). See Tables S1–S3 [26] for details of the fitting parameters.

Figure 1(h) shows that the ADMR amplitude depends strongly on H at all temperatures. However, since the magnetization of the LCO saturates above $H \sim 1$ T in the FM phase [26,67], no variation of the ADMR amplitude is expected for $H > 1$ T [7]. Besides, our measurements show a smooth change of the ADMR amplitude across the FM-PM transition, with a significant magnetoresistance measured even far above T_c [see Figs. 1(g) and 1(h)]. In contrast, a sudden drop in the magnetoresistance is expected to take place when the film becomes PM. All these observations indicate that the magnetic response of the surface of the LCO film is decoupled from its bulk.

For a better understanding of the origin of the magnetoresistance we measure the longitudinal field-dependent magnetoresistance (FDMR) along the three main axes of the sample and for different temperatures. Figures 2(a) and 2(b) show representative FDMR curves obtained far above (200 K) and below (70 K) T_c. The data indicate that the magnetoresistance in each regime should have different origins. For $T \gg T_c$, the FDMR along the y direction (i.e., the direction of the polarization of the spin accumulation in Pt) is rather constant, whereas equal paraboliclike FDMR curves are obtained in the x and z directions. This behavior is characteristic of the HMR effect in thin films with strong spin-orbit coupling [74].

For $T < T_c$, the three FDMR curves lie on the same resistance value at $H = 0$ [Fig. 2(b)]. When the magnetic field is increased, a magnetoresistance symmetric with H develops, having equal positive amplitudes in the x and z directions, and a smaller and negative amplitude in the y direction. Moreover, no hysteresis is observed between the trace and retrace curves. These observations are in sharp contrast with those found in other magnetic systems, such as YIG [5,8–10,74] and $CoFe_2O_4$ [48], where the FM order results in hysteretic FDMR curves and different resistance states around $H = 0$ for different field directions. Therefore, the FDMR measurements shown in Fig. 2(b) do not reflect the bulk FM properties of the LCO film and support the idea that the surface is magnetically decoupled.

From Fig. 2(b), we can see that the total magnetoresistance $\frac{\Delta\rho}{\rho_0} = \frac{\rho(H_z)-\rho(H_y)}{\rho_0} \cong \frac{\rho(H_x)-\rho(H_y)}{\rho_0}$ (i.e., the ADMR amplitude, Fig. 1) has two contributions: $\frac{\Delta\rho_\perp}{\rho_0} = \frac{\rho(H_z)-\rho(0)}{\rho_0} \cong \frac{\rho(H_x)-\rho(0)}{\rho_0}$ and $\frac{\Delta\rho_\parallel}{\rho_0} = \frac{\rho(0)-\rho(H_y)}{\rho_0}$. In the high-temperature regime [Fig. 2(a)], $\frac{\Delta\rho}{\rho_0} \cong \frac{\Delta\rho_\perp}{\rho_0}$ and $\frac{\Delta\rho_\parallel}{\rho_0} \approx 0$, which is consistent with HMR [74]. At low temperatures, however, we observe a finite contribution from $\frac{\Delta\rho_\parallel}{\rho_0}$ [Fig. 2(b)]. As we will demonstrate below, this contribution emerges from the magnetic response of the LCO/Pt interface. Figure 2(c) shows the temperature dependence of $\frac{\Delta\rho_\parallel}{\rho_0}$ at $H_y = 9$ T. This contribution is larger at low temperatures, decreases monotonically with increasing temperature, and drops below our resolution limit at $T \sim 125$–150 K, far above T_c. Therefore, one cannot attribute the suppression of $\frac{\Delta\rho_\parallel}{\rho_0}$ merely to the FM-PM transition of the bulk LCO film. This temperature dependence is yet another strong evidence that the magnetic response of the LCO/Pt interface must be decoupled from the bulk of the LCO film.

High-resolution STEM imaging of the cross section of the heterostructure reveals that the surface of LCO is amorphized upon deposition of Pt, forming an ultrathin $\lesssim 0.5$-nm Co-rich layer at the interface with Pt, which is disconnected from the epitaxial LCO film by a ∼1-nm-thick La/O-rich layer (see Fig. 3 and Ref. [26]). These observations support the existence of a magnetically decoupled layer at the surface of LCO, whose dimensionality and nature is also compatible with no long-range magnetic order as inferred from the SMR measurements. Amorphization of the surface of crystals upon sputter deposition of metals or semiconductors has already been observed [54,78–80], but its presence in magnetotransport experiments has been overlooked most likely because it did not result in any unexpected behavior. From the elemental profiles across the heterostructure [Fig. 3(c)], we infer that the interfusion of Co-Pt at the LCO/Pt interface, if any, must be below 1 nm (spatial resolution of the spectroscopic analysis). In this regard, note that the magnetotransport measurements

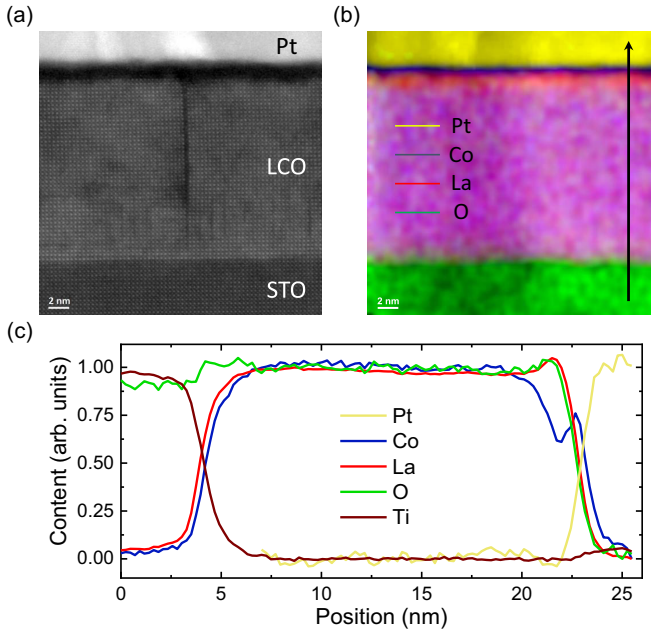

FIG. 3. (a) High-resolution HAADF STEM image of the cross section of the STO/LCO(19 nm)/Pt(5 nm) heterostructure. (b) Color-coded representation of the Pt, O, Co, and La content across the heterostructure. (c) Line scan along the black arrow in (b) indicating the spatial distribution of all the elements that constitute the heterostructure. Data in (b) and (c) are extracted by a combined spatially resolved EELS and HAADF STEM data analysis.

do not show any signature of anisotropic magnetoresistance for T $\gtrsim$ 30 K [red dots in Fig. 1(g)]. This is a compelling indication that there is no diffusion of Co into Pt, and that the Co-rich LCO layer behaves as a magnetic insulator.

Modeling. All the results presented above indicate that the Co-rich LCO surface does not exhibit long-range FM order, but a remarkable PM-like behavior. Spin-dependent phenomena, including spin pumping and the spin Seebeck effect, have been recently reported using PM materials and ascribed to the presence of short-range FM correlations [81,82]. However, current existing theories on SMR only consider long-range ferromagnetic ordering of the MI [7,72]. Here, we present a generalized theoretical model that describes the magnetoresistance in MI/NM bilayers including both SMR [7,72] and HMR [73,74] effects, as well as allows different magnetic orderings in the MI by describing microscopically the spin transport across the interface.

We model the MI/NM interface (x-y plane) as an ensemble of localized moments with spin $\mathbf{S}$. These moments interact with the conduction electrons via an exchange term $\mathcal{H} = -J_{sd}\sum_j \mathbf{S}_j \cdot \mathbf{s}(\mathbf{r}_j)$, where J_{sd} is the s-d exchange coupling and $\mathbf{s}(\mathbf{r}_j)$ is the spin density of the itinerant electrons at the position of the local moment $\mathbf{S}_j$. The spin current at the MI/NM interface is given by [26]

$$-e\mathbf{J}_{s,z} = G_s\boldsymbol{\mu}_s + G_r\mathbf{n}\times[\mathbf{n}\times\boldsymbol{\mu}_s] + G_i\mathbf{n}\times\boldsymbol{\mu}_s, \qquad (1)$$

where $e > 0$ is the elementary charge, $\mathbf{J}_{s,z}$ is the spin current flowing in the z direction, $\boldsymbol{\mu}_s$ the vector spin accumulation, and $\mathbf{n}$ a unit vector in the direction of the applied magnetic field $\mathbf{B} = \mu\mathbf{H}$, with $\mu \approx \mu_0$ the magnetic permeability of the NM layer. The parameters $G_{r,i,s}$ are obtained in the Born approximation and are defined in terms of spin averages [26,83],

$$\begin{aligned} G_r &= \frac{\pi(\nu J_{sd})^2 e^2 n_s}{\hbar}\left(\langle S_\parallel^2\rangle - \frac{\langle S_\perp^2\rangle}{2}\right),\\ G_i &= -\frac{\nu J_{sd} e^2 n_s}{\hbar}\langle S_\parallel\rangle,\\ G_s &= -\frac{\pi(\nu J_{sd})^2 e^2 n_s}{\hbar}\langle S_\perp^2\rangle, \end{aligned} \qquad (2)$$

where ν is the density of electronic states per spin species in the NM, n_s is the surface density of localized magnetic moments at the MI/NM interface, and $\hbar$ the reduced Planck constant. $S_{\parallel,\perp}$ are the components of the spin operator parallel and perpendicular to $\mathbf{H}$. The dependence of the averages $\langle S^2_{\parallel,\perp}\rangle$ and $\langle S_\parallel\rangle$ with $\mathbf{H}$ and T are determined by the type of magnetic order at the interface and, for instance, can be computed analytically for a PM.

In order to compute the magnetoresistance, we solve the spin diffusion equation in the NM layer subjected to the boundary condition imposed by Eq. (1) at the MI/NM interface and vanishing spin current at the interface with vacuum [7,72,74], and obtain the general expression for the longitudinal resistivity in leading order of $\theta_{\rm SH}$: $\rho_{\rm L} = \frac{1}{\sigma_0} + \Delta\rho_0 + \Delta\rho_1(1-n_y^2)$. Here, n_y is the y component of $\mathbf{n}$, $\sigma_0 = 1/\rho_0$ is the conductivity of the NM layer, and the corrections $\Delta\rho_{0,1}$ are given by

$$\begin{aligned} \Delta\rho_0 &= \frac{2\theta_{\rm SH}^2}{\sigma_0}\left(1 - \frac{\lambda}{d_{\rm N}}\frac{\tanh\left(\frac{d_{\rm N}}{2\lambda}\right) - \frac{G_s\lambda}{\sigma_0}}{1 - 2\frac{G_s\lambda}{\sigma_0}\coth\frac{d_{\rm N}}{\lambda}}\right),\\ \Delta\rho_1 &= \frac{2\theta_{\rm SH}^2}{\sigma_0}\left\{\frac{\lambda}{d_{\rm N}}\frac{\tanh\left(\frac{d_{\rm N}}{2\lambda}\right) - \frac{G_s\lambda}{\sigma_0}}{1 - 2\frac{G_s\lambda}{\sigma_0}\coth\frac{d_{\rm N}}{\lambda}}\right.\\ &\quad\left. - \Re\left[\frac{\Lambda}{d_{\rm N}}\frac{\tanh\left(\frac{d_{\rm N}}{2\Lambda}\right) + \frac{G\Lambda}{\sigma_0}}{1 + 2\frac{G\Lambda}{\sigma_0}\coth\frac{d_{\rm N}}{\Lambda}}\right]\right\}, \end{aligned} \qquad (3)$$

where $\frac{1}{\Lambda} = \sqrt{\frac{1}{\lambda^2} + i\frac{1}{\lambda_m^2}}$ with $\lambda_m = \sqrt{\frac{D\hbar}{g\mu_B|B|}}$, D the diffusion coefficient, g the gyromagnetic factor, μ_B the Bohr magneton, and $G = (G_r - G_s + iG_i)$.

Equations (3) generalize the magnetoresistance in MI/NM bilayers in two ways: (i) They include the effective spin conductance G_s, so far omitted in SMR, which accounts for the fact that not all magnetic moments at the MI/NM interface may align in the field direction and hence the correlation $\langle S_\perp^2\rangle$ becomes finite. In the limit $G_s \to 0$, these equations recover both the previously reported SMR and HMR corrections [7,74], merged in a single analytical expression. (ii) They contain implicitly information about the magnetic response of the MI through the temperature and field dependence of the spin conductances defined in Eqs. (2). Note that G_s is related to the ability of the spin accumulation to emit magnons in the MI and enters in Eq. (3) correcting G_r as $G_r - G_s$, which stands for the effective spin relaxation at the interface. The implications of Eqs. (2) and (3) are multiple. For instance, they can be used for understanding the temperature dependence of the SMR [84–86] or accurately describing the field dependence of the magnetoresistance for noncollinear or

nonsaturated magnets. Particularly interesting is that Eqs. (2) and (3) are also valid across magnetic phases transitions [49,53,87,88]. Furthermore, note that Eq. (2) is not restricted to SMR only, but can also be applied to describe other spin transport phenomena involving interfaces such as electrical magnon excitation [52,89–92], spin pumping [4,81,89,93,94], or the spin Seebeck effect [4,82,95,96]. See Ref. [26] for an additional discussion.

Experimental fits and discussion. We now use the above equations to describe the magnetotransport in LCO/Pt and determine the magnetic properties of the ultrathin Co-rich surface layer. Our transport measurements indicate that the Co-rich surface behaves like a PM with a large effective spin, which is compatible with the behavior of a low-dimensional isotropic Heisenberg FM, a system that exhibits short-range FM correlations with $T_c = 0$ [97]. For the fitting of the experimental data, we computed the spin correlations $\langle S^2_{\parallel,\perp}\rangle$ and $\langle S_\parallel\rangle$ that enter Eqs. (2) using the well-established random phase approximation [98], considered that the Co atoms of the surface layer can exhibit either two-dimensional (2D) or one-dimensional (1D) FM exchange coupling J, that S can be any of the possible ones in the d shell (except 0 and ½, which result in no magnetoresistance correction), considered different spin surface coverages n_s, and assumed collinear s-d exchange coupling given that $\rho(H_x) \approx \rho(H_z)$ [Fig. 2(b)] [26]. D was calculated using Einstein's relation $D = 1/2e^2\nu\rho$, and θ_{SH} and λ of Pt were estimated from the measured $\rho(T)$ [26,99]. Excellent fits to the FDMR measurements were found for a large range of parameters, some of which are summarized in Tables S1 and S2 in the Supplemental Material [26]. Figures 2(a) and 2(b) show representative fits of the data, evidencing the extraordinary good agreement with the experiment (see also Fig. S6 [26]).

The temperature dependence of $\frac{\Delta\rho_\parallel}{\rho_0}(T)$ provides additional information about the magnetic ordering of the LCO surface through $G_s(\langle S^2_\perp\rangle)$. Figure 2(c) shows the best fits obtained for the experimental data $\frac{\Delta\rho_\parallel}{\rho_0}(T)$ modeling the Co-rich LCO surface as a 2D Heisenberg magnet, a plane of spin chains, and a plane of interacting spin chains (spin ladders), all with FM coupling between spins. We also consider the case of a superparamagnet (SPM), which is described by exhibiting zero Heisenberg exchange coupling and large effective S. Our analysis evidences that a SPM cannot describe the temperature dependence of the magnetoresistance in LCO/Pt and confirms our assumption that the Co-rich surface of LCO behave as a low-dimensional Heisenberg FM [see Fig. 2(c)]. Although we cannot unambiguously distinguish between the 1D and 2D FM cases from the magnetoresistance measurements, our analysis suggests that the ultrathin Co-rich LCO layer exhibits both contributions because the temperature dependence is fitted best by the model of spin ladders [blue line, Fig. 2(c)].

Conclusions. The SMR measurements and TEM characterization of the STO/LCO/Pt structures provide clear evidence that the LCO film presents a Co-rich surface upon deposition of Pt that is magnetically decoupled from its bulk and shows no-long range FM order. Our microscopic model of the magnetoresistance in MI/NM bilayers, which revises the current SMR theory by introducing G_s, and integrates both SMR and HMR contributions in the same set of analytical equations, can explain the experimental results assuming that the surface behaves as a low-dimensional Heisenberg FM. Our theory provides a simple way to correlate the magnetic properties of the MI through the spin conductances $G_{r,i,s}$ while covering a wide range of the magnetic order, sets the base for a better understanding of diverse spin transport phenomena involving MI/NM interfaces—and their manifestation on transport properties—as well as can help to address questions related to quantum magnetism or skyrmions.

Acknowledgments. We thank Emilio Artacho for fruitful discussions. This work was supported by the European Union 7th Framework Programme under the Marie Curie Actions (607904-13-SPINOGRAPH), the European Research Council (257654-SPINTROS), and the European Regional Development Fund (ERDF), by the Spanish Ministry of Economy, Industry and Competitiveness (MINECO) (under the Maria de Maeztu Units of Excellence Programm, reference MDM-2016-0618, and under Projects MAT2015-65159-R, FIS2014-55987-P, MAT2013-46593-C6-4-P, MAT2016-80762-R, FIS2017-82804-P, and RTI2018-094861-B-100), by the Basque Government (UPV/EHU Projects IT-756-13 and IT-621-13), by the Regional Council of Gipuzkoa (100/16), and by the Xunta de Galicia (Centro singular de investigación de Galicia accreditation 2016–2019, ED431G/09). J.M.G.-P. thanks the Spanish MINECO for support by a Ph.D. fellowship (Grant No. BES-2016-077301).

[1] S. Maekawa and T. Shinjo, *Spin Dependent Transport in Magnetic Nanostructures* (Taylor and Francis, New York, 2002).

[2] A. Kobs, S. Heße, W. Kreuzpaintner, G. Winkler, D. Lott, P. Weinberger, A. Schreyer, and H. P. Oepen, Phys. Rev. Lett. **106**, 217207 (2011).

[3] A. Kobs and H. P. Oepen, Phys. Rev. B **93**, 014426 (2016).

[4] M. Weiler, M. Althammer, M. Schreier, J. Lotze, M. Pernpeintner, S. Meyer, H. Huebl, R. Gross, A. Kamra, J. Xiao, Y.-T. Chen, H. J. Jiao, G. E. W. Bauer, and S. T. B. Goennenwein, Phys. Rev. Lett. **111**, 176601 (2013).

[5] H. Nakayama, M. Althammer, Y.-T. Chen, K. Uchida, Y. Kajiwara, D. Kikuchi, T. Ohtani, S. Geprägs, M. Opel, S. Takahashi, R. Gross, G. E. W. Bauer, S. T. B. Goennenwein, and E. Saitoh, Phys. Rev. Lett. **110**, 206601 (2013).

[6] C. Hahn, G. de Loubens, O. Klein, M. Viret, V. V. Naletov, and J. Ben Youssef, Phys. Rev. B **87**, 174417 (2013).

[7] Y.-T. Chen, S. Takahashi, H. Nakayama, M. Althammer, S. T. B. Goennenwein, E. Saitoh, and G. E. W. Bauer, Phys. Rev. B **87**, 144411 (2013).

[8] N. Vlietstra, J. Shan, V. Castel, B. J. van Wees, and J. Ben Youssef, Phys. Rev. B **87**, 184421 (2013).

[9] N. Vlietstra, J. Shan, V. Castel, J. Ben Youssef, G. E. W. Bauer, and B. J. van Wees, Appl. Phys. Lett. **103**, 032401 (2013).

[10] M. Althammer, S. Meyer, H. Nakayama, M. Schreier, S. Altmannshofer, M. Weiler, H. Huebl, S. Geprägs, M. Opel, R. Gross, D. Meier, C. Klewe, T. Kuschel, J.-M. Schmalhorst, G. Reiss, L. Shen, A. Gupta, Y.-T. Chen, G. E. W. Bauer, E. Saitoh, and S. T. B. Goennenwein, Phys. Rev. B **87**, 224401 (2013).

[11] M. Isasa, A. Bedoya-Pinto, S. Vélez, F. Golmar, F. Sanchez, L. E. Hueso, J. Fontcuberta, and F. Casanova, Appl. Phys. Lett. **105**, 142402 (2014).

[12] T. Kosub, S. Vélez, J. M. Gomez-Perez, L. E. Hueso, J. Faßbender, F. Casanova, and D. Makarov, Appl. Phys. Lett. **113**, 222409 (2018).

[13] C. O. Avci, K. Garello, A. Ghosh, M. Gabureac, S. F. Alvarado, and P. Gambardella, Nat. Phys. **11**, 570 (2015).

[14] C. O. Avci, K. Garello, J. Mendil, A. Ghosh, N. Blasakis, M. Gabureac, M. Trassin, M. Fiebig, and P. Gambardella, Appl. Phys. Lett. **107**, 192405 (2015).

[15] C. O. Avci, J. Mendil, G. S. D. Beach, and P. Gambardella, Phys. Rev. Lett. **121**, 087207 (2018).

[16] H. Nakayama, Y. Kanno, H. An, T. Tashiro, S. Haku, A. Nomura, and K. Ando, Phys. Rev. Lett. **117**, 116602 (2016).

[17] J. Kim, P. Sheng, S. Takahashi, S. Mitani, and M. Hayashi, Phys. Rev. Lett. **116**, 097201 (2016).

[18] M. Althammer, J. Phys. D: Appl. Phys. **51**, 313001 (2018).

[19] M. I. Dyakonov and V. I. Perel, Phys. Lett. A **35**, 459 (1971).

[20] J. E. Hirsch, Phys. Rev. Lett. **83**, 1834 (1999).

[21] A. Hoffmann, IEEE Trans. Magn. **49**, 5172 (2013).

[22] J. Sinova, S. O. Valenzuela, J. Wunderlich, C. H. Back, and T. Jungwirth, Rev. Mod. Phys. **87**, 1213 (2015).

[23] V. M. Edelstein, Solid State Commun. **73**, 233 (1990).

[24] A. Manchon, H. C. Koo, J. Nitta, S. M. Frolov, and R. A. Duine, Nat. Mater. **14**, 871 (2015).

[25] X. Jia, K. Liu, K. Xia, and G. E. W. Bauer, Europhys. Lett. **96**, 17005 (2011).

[26] See Supplemental Material at http://link.aps.org/supplemental/10.1103/PhysRevB.100.180401 for additional measurements, discussion regarding the SMR as probe for surface magnetization, further details regarding the microscopic modeling of the magnetoresistance and applicability of the model, fitting of the experimental data, and the formal derivation of Eqs. (1) and (2), which include Refs. [27–47].

[27] N. Biškup, J. Salafranca, V. Mehta, M. P. Oxley, Y. Suzuki, S. J. Pennycook, S. T. Pantelides, and M. Varela, Phys. Rev. Lett. **112**, 087202 (2014).

[28] M.-H. Nguyen, D. C. Ralph, and R. A. Buhrman, Phys. Rev. Lett. **116**, 126601 (2016).

[29] H. Y. T. Nguyen, W. P. Pratt, Jr., and J. Bass, J. Magn. Magn. Mater. **361**, 30 (2014).

[30] E. Sagasta, Y. Omori, S. Vélez, R. Llopis, C. Tollan, A. Chuvilin, L. E. Hueso, M. Gradhand, Y. Otani, and F. Casanova, Phys. Rev. B **98**, 060410(R) (2018).

[31] H. Gamou, J. Ryu, M. Kohda, and J. Nitta, Appl. Phys. Express **10**, 023003 (2017).

[32] J. Ryu, M. Kohda, and J. Nitta, Phys. Rev. Lett. **116**, 256802 (2016).

[33] R. Freeman, A. Zholud, Z. Dun, H. Zhou, and S. Urazhdin, Phys. Rev. Lett. **120**, 067204 (2018).

[34] H. J. Jao and G. E. W. Bauer, Phys. Rev. Lett. **110**, 217602 (2013).

[35] J.-C. Rojas-Sanchez, N. Reyren, P. Laczkowski, W. Savero, J.-P. Attané, C. Deranlot, M. Jamet, J.-M. George, L. Vila, and H. Jaffrès, Phys. Rev. Lett. **112**, 106602 (2014).

[36] K. Chen and S. Zhang, Phys. Rev. Lett. **114**, 126602 (2015).

[37] K. D. Belashchenko, A. A. Kovalev, and M. van Schilfgaarde, Phys. Rev. Lett. **117**, 207204 (2016).

[38] L. Ronding, J.-P. Tetienne, T. Hingant, J.-F. Roch, P. Maletinsky, and V. Jacques, Rep. Prog. Phys. **77**, 056503 (2014).

[39] M. W. Wu, J. H. Jiang, and M. Q. Weng, Phys. Rep. **493**, 61 (2010).

[40] C. P. Slichter, *Principles of Magnetic Resonance* (Springer, Berlin, 1980).

[41] H. Callen, Phys. Rev. **130**, 890 (1963).

[42] D. A. Yablonskiy, Phys. Rev. B **44**, 4467 (1991).

[43] G. Giuliani and G. Vignale, *Quantum Theory of the Electron Liquid* (Cambridge University Press, Cambridge, U.K., 2005).

[44] V. G. Vaks, A. I. Larkin, and S. A. Pikin, Zh. Eksp. Teor. Phys. **53**, 1089 (1967) [Sov. Phys. JETP **26**, 647 (1968)].

[45] Y. A. Izyumov and Y. N. Skryabin, *Statistical Mechanics of Magnetically Ordered Systems* (Consultants Bureau, New York, 1988).

[46] Y. A. Izyumov, N. I. Chaschin, and V. Y. Yushankhai, Phys. Rev. B **65**, 214425 (2002).

[47] E. Strambini, V. N. Golovach, G. De Simoni, J. S. Moodera, F. S. Bergeret, and F. Giazotto, Phys. Rev. Mater. **1**, 054402 (2017).

[48] M. Isasa, S. Vélez, E. Sagasta, A. Bedoya-Pinto, N. Dix, F. Sánchez, L. E. Hueso, J. Fontcuberta, and F. Casanova, Phys. Rev. Applied **6**, 034007 (2016).

[49] A. Aqeel, N. Vlietstra, J. A. Heuver, G. E. W. Bauer, B. Noheda, B. J. van Wees, and T. T. M. Palstra, Phys. Rev. B **92**, 224410 (2015).

[50] A. Aqeel, N. Vlietstra, A. Roy, M. Mostovoy, B. J. van Wees, and T. T. M. Palstra, Phys. Rev. B **94**, 134418 (2016).

[51] K. Ganzhorn, J. Barker, R. Schlitz, B. A. Piot, K. Ollefs, F. Guillou, F. Wilhelm, A. Rogalev, M. Opel, M. Althammer, S. Geprägs, H. Huebl, R. Gross, G. E. W. Bauer, and S. T. B. Goennenwein, Phys. Rev. B **94**, 094401 (2016).

[52] S. Vélez, A. Bendoya-Pinto, W. Yan, L. E. Hues, and F. Casanova, Phys. Rev. B **94**, 174405 (2016).

[53] D. Hou, Z. Qiu, J. Barker, K. Sato, K. Yamamoto, S. Vélez, J. M. Gomez-Perez, L. E. Hueso, F. Casanova, and E. Saitoh, Phys. Rev. Lett. **118**, 147202 (2017).

[54] J. M. Gomez-Perez, S. Vélez, L. McKenzie-Sell, M. Amado, J. Herrero-Martín, J. López-López, S. Blanco-Canosa, L. E. Hueso, A. Chuvilin, J. W. A. Robinson, and F. Casanova, Phys. Rev. Applied **10**, 044046 (2018).

[55] V. G. Bhide, D. S. Rajoria, G. Rama Rao, and C. N. R. Rao, Phys. Rev. B **6**, 1021 (1972).

[56] M. A. Señarís-Rodríguez and J. B. Goodenough, J. Solid State Chem. **116**, 224 (1995).

[57] P. Ravindran, P. A. Korzhavyi, H. Fjellvag, and A. Kjekshus, Phys. Rev. B **60**, 16423 (1999).

[58] J. Androulakis, N. Katsarakis, and J. Giapintzakis, Phys. Rev. B **64**, 174401 (2001).

[59] J.-Q. Yan, J.-S. Zhou, and J. B. Goodenough, Phys. Rev. B **70**, 014402 (2004).

[60] A. M. Durand, D. P. Belanger, C. H. Booth, F. Ye, S. Chi, J. A. Fernandez-Baca, and M. Bhat, J. Phys.: Condens. Matter **25**, 382203 (2013).

[61] A. Ikeda, T. Nomura, Y. H. Matsuda, A. Matsuo, K. Kindo, and K. Sato, Phys. Rev. B **93**, 220401(R) (2016).

[62] J. Buckeridge, F. H. Taylor, and C. R. A. Catlow, Phys. Rev. B **93**, 155123 (2016).

[63] H. Hsu, P. Blaha, and R. M. Wentzcovitch, Phys. Rev. B **85**, 140404(R) (2012).

[64] D. Fuchs, E. Arac, C. Pinta, S. Schuppler, R. Schneider, and H. v. Löhneysen, Phys. Rev. B **77**, 014434 (2008).

[65] S. Park, R. Ryan, E. Karapetrova, J. W. Kim, J. X. Ma, J. Shi, J. W. Freeland, and W. Wu, Appl. Phys. Lett. **95**, 072508 (2009).

[66] W. S. Choi, J. Kwon, H. Jeen, J. E. Hamann-Borrero, A. Radi, S. Macke, R. Sutarto, F. He, G. A. Sawatzky, V. Hinkov, M. Kim, and H. N. Lee, Nano Lett. **12**, 4966 (2012).

[67] F. Rivadulla, Z. Bi, E. Bauer, B. Rivas-Murias, J. M. Vila-Fungueiriño, and Q. Jia, Chem. Mater. **25**, 55 (2013).

[68] L. Qiao, J. H. Jang, D. J. Singh, Z. Gai, H. Xiao, A. Mehta, R. K. Vasudevan, A. Tselev, Z. Feng, H. Zhou, S. Li, W. Prellier, X. Zu, Z. Liu, A. Borisevich, A. P. Baddorf, and M. D. Biegalski, Nano Lett. **15**, 4677 (2015).

[69] B. Rivas-Murias, I. Lucas, P. Jiménez-Cavero, C. Magén, L. Morellón, and F. Rivadulla, Nano Lett. **16**, 1736 (2016).

[70] Y. Yokoyama, Y. Yamasaki, M. Taguchi, Y. Hirata, K. Takubo, J. Miyawaki, Y. Harada, D. Asakura, J. Fujioka, M. Nakamura, H. Daimon, M. Kawasaki, Y. Tokura, and H. Wadati, Phys. Rev. Lett. **120**, 206402 (2018).

[71] T. Shang, Q. F. Zhan, H. L. Yang, Z. H. Zuo, Y. L. Xie, Y. Zhang, L. P. Liu, B. M. Wang, Y. H. Wu, S. Zhang, and R.-W. Li, Phys. Rev. B **92**, 165114 (2015).

[72] Y.-T. Chen, S. Takahashi, H. Nakayama, M. Althammer, S. T. B. Goennenwein, E. Saitoh, and G. E. W. Bauer, J. Phys.: Condens. Matter. **28**, 103004 (2016).

[73] M. I. Dyakonov, Phys. Rev. Lett. **99**, 126601 (2007).

[74] S. Vélez, V. N. Golovach, A. Bedoya-Pinto, M. Isasa, E. Sagasta, M. Abadia, C. Rogero, L. E. Hueso, F. S. Bergeret, and F. Casanova, Phys. Rev. Lett. **116**, 016603 (2016).

[75] A. Brataas, Y. V. Nazarov, and G. E. W. Bauer, Phys. Rev. Lett. **84**, 2481 (2000).

[76] J. Flipse, F. K. Dejene, D. Wagenaar, G. E. W. Bauer, J. Ben Youssef, and B. J. van Wees, Phys. Rev. Lett. **113**, 027601 (2014).

[77] J. Xiao and G. E. W. Bauer, arXiv:1508.02486.

[78] S. Valeri, S. Altieri, T. Di Domenico, and R. Verucchi, J. Vac. Sci. Technol. A **13**, 394 (1995).

[79] J. Lusktikova, Y. Shiomi, Z. Qiu, T. Kikkawa, R. Iguchi, K. Uchida, and E. Saitoh, J. Appl. Phys. **116**, 153902 (2014).

[80] D. Song, L. Ma, S. Zhou, and J. Zhu, Appl. Phys. Lett. **107**, 042401 (2015).

[81] Y. Shiomi and E. Saitoh, Phys. Rev. Lett. **113**, 266602 (2014).

[82] S. M. Wu, J. E. Pearson, and A. Bhattacharya, Phys. Rev. Lett. **114**, 186602 (2015).

[83] X.-P. Zhang, F. S. Bergeret, and V. N. Golovach, Nano Lett. **19**, 6330 (2019).

[84] S. Meyer, M. Althammer, S. Geprägs, and S. T. B. Goennenwein, Appl. Phys. Lett. **104**, 242411 (2014).

[85] S. R. Marmion, M. Ali, M. McLaren, D. A. Williams, and B. J. Hickey, Phys. Rev. B **89**, 220404(R) (2014).

[86] K. Uchida, Z. Qiu, T. Kikkawa, R. Iguchi, and E. Saitoh, Appl. Phys. Lett. **106**, 052405 (2015).

[87] R. Schlitz, T. Kosub, A. Thomas, S. Fabretti, K. Nielsch, D. Makarov, and S. T. B. Goennenwein, Appl. Phys. Lett. **112**, 132401 (2018).

[88] T. Lino, T. Moriyama, H. Iwaki, H. Aono, Y. Shiratsuchi, and T. Ono, Appl. Phys. Lett. **114**, 022402 (2019).

[89] Y. Kajiwara, K. Harii, S. Takahashi, J. Ohe, K. Uchida, M. Mizuguchi, H. Umezawa, H. Kawai, K. Ando, K. Takanashi, S. Maekawa, and E. Saitoh, Nature (London) **464**, 262 (2010).

[90] L. J. Cornelissen, J. Liu, R. A. Duine, J. Ben Youssef, and B. J. van Wees, Nat. Phys. **11**, 1022 (2015).

[91] S. T. B. Goennenwein, R. Schlitz, M. Pernpeintner, K. Ganzhorn, M. Althammer, R. Gross, and H. Huebl, Appl. Phys. Lett. **107**, 172405 (2015).

[92] R. Lebrun, A. Ross, S. A. Bender, A. Qaiumzadeh, L. Baldrati, J. Cramer, A. Brataas, R. A. Duine, and M. Kläui, Nature (London) **561**, 222 (2018).

[93] Y. Tserkovnyak, A. Brataas, G. E. W. Bauer, and B. I. Halperin, Rev. Mod. Phys. **77**, 1375 (2005).

[94] E. Saitoh, M. Ueda, H. Miyajima, and G. Tatara, Appl. Phys. Lett. **88**, 182509 (2006).

[95] K. Uchida, J. Xiao, H. Adachi, J. Ohe, S. Takahashi, J. Ieda, T. Ota, Y. Kajiwara, H. Umezawa, H. Kawai, G. E. W. Bauer, S. Maekawa, and E. Saitoh, Nat. Mater. **9**, 894 (2010).

[96] S. Geprägs, A. Kehlberger, F. Della Coletta, Z. Qiu, E.-J. Guo, T. Schulz, C. Mix, S. Meyer, A. Kamra, M. Althammer, H. Huebl, G. Jakob, Y. Ohnuma, H. Adachi, J. Barker, S. Maekawa, G. E. W. Bauer, E. Saitoh, R. Gross, S. T. B. Goennenwein, and M. Kläui, Nat. Commun. **7**, 10452 (2016).

[97] N. D. Mermin and H. Wagner, Phys. Rev. Lett. **17**, 1133 (1966).

[98] N. Majlis, *The Quantum Theory of Magnetism*, 2nd ed. (World Scientific, Singapore, 2007).

[99] E. Sagasta, Y. Omori, M. Isasa, M. Gradhand, L. E. Hueso, Y. Niimi, Y. C. Otani, and F. Casanova, Phys. Rev. B **94**, 060412(R) (2016).